Intermittency in coupled maps

Sang-Yoon Kim *
Department of Physics
Kangwon National University
Chunchon, Kangwon-Do 200-701, Korea

Abstract

Using a renormalization method, we study the critical behavior for intermittency in two coupled one-dimensional (1D) maps. We find two fixed maps of the renormalization transformation. They all have common relevant eigenvalues associated with scaling of the control parameter of the uncoupled 1D map. However, the relevant "coupling eigenvalues" associated with coupling perturbations vary depending on the fixed maps. It is also found that the two fixed maps are associated with the critical behavior in the vicinity of a critical line segment. One fixed map with no relevant coupling eigenvalues governs the critical behavior at interior points of the critical line segment, while the other one with relevant coupling eigenvalues governs the critical behavior at both ends. The results of the two coupled 1D maps are also extended to many globally-coupled 1D maps, in which each 1D map is coupled to all the other ones with equal strength.

PACS numbers : 05.45.+b, 03.20.+i, 05.70.Jk

*Electronic address: sykim@cc.kangwon.ac.kr

I. INTRODUCTION

An intermittent transition to chaos in the 1D map occurs in the vicinity of a saddle-node bifurcation [1]. Intermittency just preceding a saddle-node bifurcation to a periodic attractor is characterized by the occurrence of intermittent alternations between laminar and turbulent behaviors. Scaling relations for the average duration of laminar behavior in the presence of noise have been first established [2] by considering a Langevin equation describing the map near the intermittency threshold and using Fokker-Plank techniques. The same scaling results have been later found [3] by using the same renormalization-group equation [4] for period doubling with a mere change of boundary conditions appropriate to a saddle-node bifurcation.

Recently, efforts have been made to generalize the scaling results of period doubling for the 1D map to coupled 1D maps [5–11], which are used to simulate spatially extended systems with effectively many degrees of freedom [12]. It has been found that the critical scaling behaviors of period doubling for the coupled 1D maps are much richer than those for the uncoupled 1D map [8–11]. These results for the abstract system of the coupled 1D maps are also confirmed in the real system of the coupled oscillators [13]. In a similar way, the scaling results of the higher period p-tuplings ($p =, 3, 4, ...$) in the 1D map are also generalized to the coupled 1D maps [14]. Here we are interested in another route to chaos via intermittency in coupled 1D maps. Using a renormalization method, we extend the scaling results of intermittency for the 1D map to coupled 1D maps.

This paper is organized as follows. In Sec. II we introduce two coupled 1D maps and discuss their symmetry. Bifurcations associated with stability of periodic orbits are also discussed there. In Sec. III we employ the same renormalization method [10] developed for period doubling in coupled 1D maps and study the critical behavior for intermittency in two coupled 1D maps. We thus find two fixed maps of the renormalization transformation. They have the relevant eigenvalues associated with scaling of the control parameter of the uncoupled 1D map as common ones. However, the relevant "coupling eigenvalues" (CE's) associated with coupling perturbations vary depending on the fixed maps. These two fixed maps are also found to be associated with the critical behavior near a critical line segment in Sec. IV. One fixed map with no relevant CE's governs the critical behavior at interior points of the critical line, while the other one with relevant CE's governs the critical behavior at both end points. We also study the critical behavior for intermittency in many globally-coupled 1D maps in Sec. V. Globally-coupled systems, in which each element is coupled to all the other ones with equal strength, appear naturally in broad branches of science [15]. The results of two coupled maps are extended to this kind of many globally-coupled maps. Finally, a summary is given in Sec. VI.

II. TWO COUPLED 1D MAPS

After briefly reviewing the intermittency in case of the 1D map, we introduce two coupled 1D maps and discuss their symmetry. Bifurcations associated with stability of periodic orbits are also discussed.

We first recapitulate the intermittent transition to chaos [1–3] in a 1D map with one control parameter A, $X_{t+1} = u(X_t)$ (t denotes a discrete time). A pair of orbits with period p

appears via saddle-node bifurcation, as the control parameter A exceeds a threshold value A_c. One periodic orbit is a stable attractor, while the other one is an unstable repeller. However, as A decreases below A_c, the two periodic orbits disappear, and an intermittent chaotic attractor, characterized by the occurrence of intermittent alternations between laminar and turbulent behaviors, appears.

One can easily explain the intermittency geometrically as follows. The curve of the equation $Y = u^{(p)}(X)$ [$u^{(p)}$ is the pth iterate of u] has new $2p$ intersection points with the $Y = X$ line for $A > A_c$, which collapse into p points tangent to the $Y = X$ line for $A = A_c$ (i.e., we have p fixed points, $X_t^* = u^{(p)}(X_t^*)$, $t = 1, \ldots, p$ for $A = A_c$). However, as A decreases below A_c the curve no longer touches the $Y = X$ line so that a "channel" appears in the immediate vicinity of each point tangent to the $Y = X$ line at $A = A_c$. If one orbit point falls close to the entrance to one of the channels under repeated iterations of $u^{(p)}$, it would take many iterations to go through the channel, which corresponds to the "laminar phase." After slow passage through the channel, the iterates of $u^{(p)}$ move wildly until they return to one of the channels. This corresponds to the "turbulent phase." Thus the laminar and turbulent phases appear intermittently.

The nearer A is to A_c, the longer the averaged laminar time. To obtain the average duration of the laminar phase, consider the pth iterate $u^{(p)}(X)$ in the immediate vicinity of one of the channels. Shifting the origin of coordinate X to a fixed point X^* of $u^{(p)}(X)$ for $A = A_c$, we have

$$x_{t+1} = f(x_t) \equiv u^{(p)}(x_t + X^*) - X^* \approx x_t + a|x_t|^z + \epsilon, \quad z > 1, \tag{2.1}$$

where $x = X - X^*$, a is a constant, and ϵ is a control parameter proportional to $A - A_c$. Using a map f of the form (2.1), it has been found in [3] that the mean duration of the laminar phase $\bar{l}(\epsilon)$ varies as $\epsilon^{-(1-1/z)}$. Hence the tangency-order z determines the universality classes, because $\bar{l}$ depends on the order z. In this paper, we consider only the analytic case of even order z ($z = 2, 4, 6, \ldots$).

We now consider a map M consisting of two identical 1D maps coupled symmetrically,

$$M : \begin{cases} X_{t+1} = W(X_t, Y_t) = u(X_t) + v(X_t, Y_t), \\ Y_{t+1} = W(Y_t, X_t) = u(Y_t) + v(Y_t, X_t), \end{cases} \tag{2.2}$$

where v is a coupling function obeying a condition,

$$v(X, X) = 0 \ \text{ for any } \ X. \tag{2.3}$$

The map (2.2) is called a symmetric map because it has an exchange symmetry such that

$$\sigma^{-1} M \sigma(\mathbf{Z}) = M(\mathbf{Z}) \ \text{ for all } \ \mathbf{Z}, \tag{2.4}$$

where $\mathbf{Z} = (X, Y)$, σ is an exchange operator acting on $\mathbf{Z}$ such that $\sigma(\mathbf{Z}) = (Y, X)$, and σ^{-1} is its inverse. The set of all fixed points of σ forms a synchronization line $Y = X$ in the state space. It follows from Eq. (2.4) that the exchange operator σ commutes with the symmetric map M, i.e., $\sigma M = M\sigma$. Thus the synchronization line becomes invariant under M, i.e., if a point $\mathbf{Z}$ lies on the synchronization line, then its image $M(\mathbf{Z})$ also lies on it. An

orbit is called a(n) (in-phase) synchronous orbit if it lies on the synchronization line, i.e., it satisfies

$$X_t = Y_t \equiv X_t^* \ \text{ for all } \ t. \tag{2.5}$$

Otherwise, it is called an (out-of-phase) asynchronous orbit. Here we study the intermittency associated with a saddle-node bifurcation to a pair of synchronous periodic orbits, which can be easily found from the uncoupled 1D map, $X_{t+1}^* = u(X_t^*)$, because of the coupling condition (2.3).

Stability of a synchronous orbit of period p is determined from the Jacobian matrix J of $M^{(p)}$ (pth iterate of M), which is given by the p product of the linearized map DM of the map (2.2) along the orbit

$$\begin{aligned} J &= \prod_{t=1}^{p} DM(X_t^*, X_t^*) \\ &= \prod_{t=1}^{p} \begin{pmatrix} u'(X_t^*) - V(X_t^*) & V(X_t^*) \\ V(X_t^*) & u'(X_t^*) - V(X_t^*) \end{pmatrix}, \end{aligned} \tag{2.6}$$

where $u'(x) = du(X)/dX$ and $V(X) = \partial v(X,Y)/\partial Y|_{Y=X}$; hereafter $V(X)$ will be referred to as the "reduced coupling function" of $g(x,y)$. The eigenvalues of J, called the stability multipliers of the orbit, are gievn by

$$\lambda_1 = \prod_t^p u'(X_t^*), \quad \lambda_2 = \prod_t^p [u'(X_t^*) - 2V(X_t^*)]. \tag{2.7}$$

Note that λ_1 is just the stability multiplier for the case of the uncoupled 1D map and the coupling affects only λ_2.

A synchronous periodic orbit is stable when both multipliers lie inside the unit circle, i.e., $|\lambda_j| < 1$ for $j = 1$ and 2. Thus its stable region in the parameter plane is bounded by four bifurcation lines, i.e., those curves determined by the equations $\lambda_j = \pm 1$ ($j = 1, 2$). When a multiplier λ_j increases through 1, the stable synchronous periodic orbit loses its stability via saddle-node or pitchfork bifurcation. On the other hand, when a multiplier λ_j decreases through -1, it becomes unstable via period-doubling bifurcation. (For more details on bifurcations, refer to Ref. [16].)

III. RENORMALIZATION ANALYSIS OF TWO COUPLED MAPS

Here we are interested in intermittency just preceding a saddle-node bifurcation. The intermittent transition to chaos occurs near a critical line segment, as will be seen in Sec. IV. Using the same renormalization method [10,11] for period doubling with a mere change of boundary conditions appropriate for a saddle-node bifurcation, we generalize the 1D scaling results for intermittency to the case of two coupled 1D maps. We thus find two fixed maps of the renormalization transformation and obtain their relevant eigenvalues. One fixed map is associated with the critical behavior inside the critical line, while the other one is associated with the critical behavior at both ends.

To study the intermittent transition to chaos near a saddle-node bifurcation to a pair of synchronous orbits of period p, consider the pth iterate $M^{(p)}$ of M of Eq. (2.2),

$$M^{(p)} : X_{t+1} = W^{(p)}(X_t, Y_t),\ Y_{t+1} = W^{(p)}(Y_t, X_t), \tag{3.1}$$

where $W^{(p)}$ satisfies a recurrence relation

$$W^{(p)}(X, Y) = W(W^{(p-1)}(X, Y), W^{(p-1)}(Y, X)). \tag{3.2}$$

The function $W^{(p)}$ can be decomposed into the uncoupled part $u^{(p)}$ and the remaining coupling part, i.e.,

$$W^{(p)}(X, Y) = u^{(p)}(X) + [W^{(p)}(X, Y) - u^{(p)}(X)]. \tag{3.3}$$

When the control parameter A of the uncoupled 1D map is equal to the threshold value A_c for the synchronous saddle-node bifurcation, we have p synchronous fixed points of $M^{(p)}$ such that $Y_t^* = X_t^* = u^{(p)}(X_t^*)$ for $t = 1, \ldots, p$. Shifting the origin of coordinates (X, Y) to one of the p synchronous fixed points (X^*, Y^*) ($Y^* = X^* = u^{(p)}(X^*)$ for $A = A_c$), we have

$$T : \begin{cases} x_{t+1} = F(x_t, y_t) = f(x_t) + g(x_t, y_t), \\ y_{t+1} = F(y_t, x_t) = f(y_t) + g(y_t, x_t), \end{cases} \tag{3.4}$$

where

$$f(x) = u^{(p)}(x + X^*) - X^*, \tag{3.5}$$

$$g(x, y) = W^{(p)}(x + X^*, y + Y^*) - u^{(p)}(x + X^*). \tag{3.6}$$

Since a synchronous saddle-node bifurcation occurs at the origin $(0, 0)$ for $A = A_c$ in case of the map T, the uncoupled part f for the critical case $A = A_c$ satisfies

$$f(0) = 0 \quad \text{and} \quad f'(0) = 1. \tag{3.7}$$

Note also that the coupling function $g(x, y)$ satisfies the coupling condition (2.3), i.e.,

$$g(x, x) = 0 \quad \text{for any } x. \tag{3.8}$$

We employ the same renormalization transformation [10,11] as in the period-doubling case with changed boundary conditions (3.7). The renormalization transformation $\mathcal{N}$ for a coupled map T consists of squaring (T^2) and rescaling (B) operators:

$$\mathcal{N}(T) \equiv BT^2B^{-1}. \tag{3.9}$$

Since we consider only synchronous orbits, the rescaling operator is of the form,

$$B = \begin{pmatrix} \alpha & 0 \\ 0 & \alpha \end{pmatrix}, \tag{3.10}$$

where α is a rescaling factor.

Applying the renormalization operator $\mathcal{N}$ to the coupled map (3.4) n times, we obtain the n-times renormalized map T_n of the form,

$$T_n : \begin{cases} x_{t+1} = F_n(x_t, y_t) = f_n(x_t) + g_n(x_t, y_t), \\ y_{t+1} = F_n(y_t, x_t) = f_n(y_t) + g_n(y_t, x_t). \end{cases} \tag{3.11}$$

Here f_n and g_n are the uncoupled and coupling parts of the n-times renormalized function F_n, respectively. They satisfy the following recurrence equations [10,11]:

$$f_{n+1}(x) = \alpha f_n(f_n(\frac{x}{\alpha})), \tag{3.12}$$

$$\begin{aligned} g_{n+1}(x,y) = {} & \alpha f_n(f_n(\frac{x}{\alpha}) + g_n(\frac{x}{\alpha}, \frac{y}{\alpha})) \\ & + \alpha g_n(f_n(\frac{x}{\alpha}) + g_n(\frac{x}{\alpha}, \frac{y}{\alpha}), f_n(\frac{y}{\alpha}) \\ & + g_n(\frac{y}{\alpha}, \frac{x}{\alpha})) - \alpha f_n(f_n(\frac{x}{\alpha})). \end{aligned} \tag{3.13}$$

Then Eqs. (3.12) and (3.13) define a renormalization operator $\mathcal{R}$ of transforming a pair of functions, (f, g);

$$\begin{pmatrix} f_{n+1} \\ g_{n+1} \end{pmatrix} = \mathcal{R} \begin{pmatrix} f_n \\ g_n \end{pmatrix}. \tag{3.14}$$

A critical map T_c with the nonlinearity and coupling parameters set to their critical values is attracted to a fixed map T^* under iterations of the renormalization transformation $\mathcal{N}$,

$$T^* : \begin{cases} x_{t+1} = F^*(x_t, y_t) = f^*(x_t) + g^*(x_t, y_t), \\ y_{t+1} = F^*(y_t, x_t) = f^*(y_t) + g^*(y_t, x_t). \end{cases} \tag{3.15}$$

Here (f^*, g^*) is a fixed point of the renormalization operator $\mathcal{R}$, which satisfies $(f^*, g^*) = \mathcal{R}(f^*, g^*)$. Note that the equation for f^* is just the fixed-point equation for the intermittency with boundary conditions (3.7) in the uncoupled 1D map. It has been found in [3] that

$$\begin{aligned} f^*(x) &= x[1 - (z-1)ax^{z-1}]^{-1/(z-1)} \\ &= x + ax^z + \frac{z}{2}a^2x^{2z-1} + \cdots \quad (a : \text{arbitrary constant}) \end{aligned} \tag{3.16}$$

is a fixed point of the transformation (3.12) with

$$\alpha = 2^{1/(z-1)}. \tag{3.17}$$

[As mentioned in Sec. II, we consider only the analytic case of even order z ($z = 2, 4, 6, \ldots$).] Consequently, only the equation for the coupling fixed function g^* is left to be solved.

However, it is not easy to directly solve the equation for the coupling fixed function. We therefore introduce a tractable recurrence equation for a reduced coupling function of the coupling function $g(x, y)$, defined by

$$G(x) \equiv \left. \frac{\partial g(x,y)}{\partial y} \right|_{y=x}. \tag{3.18}$$

Differentiating the recurrence equation (3.13) for g with respect to y and setting $y = x$, we have

$$G_{n+1}(x) = [f_n'(f_n(\frac{x}{\alpha})) - 2G_n(f_n(\frac{x}{\alpha}))]G_n(\frac{x}{\alpha}) + G_n(f_n(\frac{x}{\alpha}))f_n'(\frac{x}{\alpha}). \tag{3.19}$$

Then Eqs. (3.12) and (3.19) define a "reduced renormalization operator" $\tilde{\mathcal{R}}$ of transforming a pair of functions (f, G) [10,11]:

$$\begin{pmatrix} f_{n+1} \\ G_{n+1} \end{pmatrix} = \tilde{\mathcal{R}} \begin{pmatrix} f_n \\ G_n \end{pmatrix}. \tag{3.20}$$

We now look for a fixed point (f^*, G^*) of $\tilde{\mathcal{R}}$, which satisfies $(f^*, G^*) = \tilde{\mathcal{R}}(f^*, G^*)$. Here G^* is just the reduced coupling fixed function of g^* (i.e., $G^*(x) = \partial g^*(x,y)/\partial y|_{y=x}$). Using a series-expansion method, we find two solutions for G^*:

$$G_I^*(x) = \frac{1}{2}[1 + zax^{z-1} + z(z - \frac{1}{2})a^2x^{2(z-1)} + \cdots], \tag{3.21}$$

$$G_{II}^*(x) = \frac{1}{2}[bax^{z-1} + b(\frac{3z-b}{2} - \frac{1}{2})a^2x^{2(z-1)} + \cdots], \tag{3.22}$$

where a and b are arbitrary constants. Here we are able to sum the series in Eq. (3.21) and obtain a closed-form solution,

$$G_I^*(x) = \frac{1}{2}f^{*\prime}(x). \tag{3.23}$$

However, unfortunately we cannot sum the series in Eq. (3.22), except for the cases $b = 0$ and z where we obtain closed-form solutions,

$$G_{II}^*(x) = \begin{cases} 0 & \text{for } b = 0, \\ \frac{1}{2}[f^{*\prime}(x) - 1] & \text{for } b = z. \end{cases} \tag{3.24}$$

Consider an infinitesimal perturbation (h, Φ) to a fixed point (f^*, G^*) of the reduced renormalization operator $\tilde{\mathcal{R}}$. We then examine the evolution of a pair of functions $(f^* + h, G^* + \Phi)$ under $\tilde{\mathcal{R}}$. Linearizing $\tilde{\mathcal{R}}$ at its fixed point, we obtain a reduced linearized operator $\tilde{\mathcal{L}}$ transforming a pair of perturbations (h, Φ):

$$\begin{pmatrix} h_{n+1} \\ \Phi_{n+1} \end{pmatrix} = \tilde{\mathcal{L}} \begin{pmatrix} h_n \\ \Phi_n \end{pmatrix} = \begin{pmatrix} \tilde{\mathcal{L}}_1 & 0 \\ \tilde{\mathcal{L}}_3 & \tilde{\mathcal{L}}_2 \end{pmatrix} \begin{pmatrix} h_n \\ \Phi_n \end{pmatrix}, \tag{3.25}$$

where

$$h_{n+1}(x) = [\tilde{\mathcal{L}}_1 h_n](x) = \alpha f^{*\prime}(f^*(\frac{x}{\alpha}))h_n(\frac{x}{\alpha}) + \alpha h_n(f^*(\frac{x}{\alpha})), \tag{3.26}$$

$$\Phi_{n+1}(x) = [\tilde{\mathcal{L}}_2\Phi_n](x) + [\tilde{\mathcal{L}}_3 h_n](x), \tag{3.27}$$

$$[\tilde{\mathcal{L}}_2\Phi_n](x) = [f^{*\prime}(f^*(\frac{x}{\alpha})) - 2G^*(f^*(\frac{x}{\alpha}))]\Phi_n(\frac{x}{\alpha}) + [f^{*\prime}(\frac{x}{\alpha}) - 2G^*(\frac{x}{\alpha})]\Phi_n(f^*(\frac{x}{\alpha})), \tag{3.28}$$

$$[\tilde{\mathcal{L}}_3 h_n](x) = [f^{*\prime\prime}(f^*(\frac{x}{\alpha}))G^*(\frac{x}{\alpha}) - 2G^{*\prime}(f^*(\frac{x}{\alpha}))G^*(\frac{x}{\alpha}) + G^{*\prime}(f^*(\frac{x}{\alpha}))f^{*\prime}(\frac{x}{\alpha})]h_n(\frac{x}{\alpha}) + G^*(\frac{x}{\alpha})h_n'(f^*(\frac{x}{\alpha})) + G^*(f^*(\frac{x}{\alpha}))h_n'(\frac{x}{\alpha}). \tag{3.29}$$

Here the prime denotes a derivative. Note that, although h_n couples to both h_{n+1} and Φ_{n+1}, Φ_n couples only to Φ_{n+1}. From this reducibility of $\tilde{\mathcal{L}}$ into a semiblock form, it follows that to obtain the eigenvalues of $\tilde{\mathcal{L}}$ it is sufficient to solve the eigenvalue problems for $\tilde{\mathcal{L}}_1$ and $\tilde{\mathcal{L}}_2$ separately. The eigenvalues of both $\tilde{\mathcal{L}}_1$ and $\tilde{\mathcal{L}}_2$ give the whole spectrum of $\tilde{\mathcal{L}}$.

A pair of perturbations (h^*, Φ^*) is called an eigenperturbation with eigenvalue λ, if

$$\lambda \begin{pmatrix} h^* \\ \Phi^* \end{pmatrix} = \tilde{\mathcal{L}} \begin{pmatrix} h^* \\ \Phi^* \end{pmatrix}, \tag{3.30}$$

that is,

$$\lambda h^*(x) = [\tilde{\mathcal{L}}_1 h^*](x), \tag{3.31}$$

$$\lambda \Phi^*(x) = [\tilde{\mathcal{L}}_2 \Phi^*](x) + [\tilde{\mathcal{L}}_3 h^*](x). \tag{3.32}$$

We first solve Eq. (3.31) to find eigenvalues of $\tilde{\mathcal{L}}_1$. Note that this is just the eigenvalue equation for the 1D map case. The complete spectrum of eigenvalues and the corresponding eigenfunctions have been found in Refs. [3]. The form of the eigenvalues is $\lambda_n = 2^{(z-n)/(z-1)}$ $(n = 0, 1, 2, \ldots)$. Hence the first z eigenvalues with $n < z$ are relevant ones. The marginal one λ_z is associated with the arbitrary constant a in $f^*(x)$, and all the other ones with $n > z$ are irrelevant. Although the eigenvalues λ_n's of $\tilde{\mathcal{L}}_1$ are also eigenvalues of $\tilde{\mathcal{L}}$ as mentioned in the preceding paragraph, $(h^*, 0)$ itself cannot be an eigenperturbation of $\tilde{\mathcal{L}}$ unless $\tilde{\mathcal{L}}_3$ is a null operator.

We next consider a perturbation of the form $(0, \Phi)$ having only the coupling part. If a reduced coupling perturbation Φ^* satisfies

$$\begin{aligned} \lambda \Phi^*(x) &= [\tilde{\mathcal{L}}_2 \Phi^*](x) \\ &= [f^{*\prime}(f^*(\frac{x}{\alpha})) - 2G^*(f^*(\frac{x}{\alpha}))]\Phi^*(\frac{x}{\alpha}) \\ &\quad + [f^{*\prime}(\frac{x}{\alpha}) - 2G^*(\frac{x}{\alpha})]\Phi^*(f^*(\frac{x}{\alpha})), \end{aligned} \tag{3.33}$$

then it is called a reduced coupling eigenperturbation with coupling eigenvalue (CE) λ. In this case $(0, \Phi^*)$ becomes an eigenperturbation of $\tilde{\mathcal{L}}$ with CE λ.

We first consider the case of the solution $G_I^*(x) = \frac{1}{2} f^{*\prime}(x)$. In this case the linearized operator $\tilde{\mathcal{L}}_2$ of Eq. (3.33) becomes a null operator because the right-hand side of the equation becomes zero. Hence there exist no relevant CE's associated with coupling perturbations, and consequently the fixed point (f^*, G_I^*) has only relevant eigenvalues of $\tilde{\mathcal{L}}_1$ associated with scaling of the control parameter of the uncoupled 1D map. As will be seen in Sec. IV, the intermittent transition to chaos occurs near a critical line segment. The critical behaviors near interior points of the critical line segment are essentially the same as those for the 1D case. In fact, a pair of critical functions (f_c, G_c) at any interior point is attracted to the same fixed point (f^*, G_I^*) under iterations of $\tilde{\mathcal{R}}$. Hence the fixed point (f^*, G_I^*) governs the critical behaviors inside the critical line segment. (For details refer to the next section.)

Second, consider the case of the solution G_{II}^* of Eq. (3.22). Using a series-expansion method, we find the complete spectrum of CE's and the corresponding eigenfunctions. An eigenfunction $\Phi^*(x)$ can be expanded as follows:

$$\Phi^*(x) = \sum_{l=0}^{\infty} c_l \, x^l. \tag{3.34}$$

Substituting the power series of $f^*(x)$, $f^{*\prime}(x)$, $G^*_{II}(x)$ and $\Phi^*(x)$ into the eigenvalue equation (3.33), it has the structure

$$\lambda\, c_k \;=\; \sum_l \mathcal{M}_{kl}\, c_l, \quad k, l = 0, 1, 2, \ldots \ . \tag{3.35}$$

Note that each c_l ($l = 0, 1, 2, \ldots$) in the right-hand side is involved only in the determination of coefficients of monomials x^k with $k = l + m(z-1)$ ($m = 0, 1, 2, \ldots$). Hence $\mathcal{M}$ becomes a lower triangular matrix. Its eigenvalues are therefore just diagonal elements:

$$\lambda_k = \mathcal{M}_{kk} = \frac{2}{\alpha^k} = 2^{(z-1-k)\,/\,(z-1)}, \quad k = 0, 1, 2, \ldots \ . \tag{3.36}$$

The first $(z-1)$ eigenvalues λ_k's for $0 \le k \le z-2$ are relevant ones. The marginal eigenvalue λ_{z-1} is associated with the arbitrary constant b in $G^*_{II}(x)$, and all the other eigenvalues for $k > z-1$ are irrelevant.

Each eigenfunction $\Phi^*_k(x)$ with CE λ_k ($k = 0, 1, 2, \ldots$) is of the form,

$$\Phi^*_k(x) = x^k[1 + (z - b + \frac{k}{2})ax^{z-1} + \cdots]. \tag{3.37}$$

In case of the largest CE $\lambda_0 = 2$, we are able to sum the series in Eq. (3.37) for $b = 0$ and z and find $\Phi^*_0(x)$ in closed form:

$$\Phi^*_0(x) = \begin{cases} f^{*\prime}(x) & \text{for } b = 0, \\ 1 & \text{for } b = z. \end{cases} \tag{3.38}$$

We can also sum the series in Eq. (3.37) for all the irrelevant cases (i.e., the cases $k \ge z$) and find the closed-form eigenfunctions,

$$\Phi^*_k(x) = \frac{1}{al}[f^{*\prime}(x) - 2G^*_{II}(x)][f^{*l}(x) - x^l], \quad l = k - z + 1 = 1, 2, \ldots \ , \tag{3.39}$$

which are associated with coordinate changes [17].

As we shall see in the next section IV, the second reduced coupling function $G^*_{II}(x)$ governs the critical behavior near both ends of a critical line segment, because a pair of critical functions (f_c, G_c) at each end point is attracted to the fixed point (f^*, G^*_{II}) under iterations of $\tilde{\mathcal{R}}$. (For details refer to the next section.)

IV. SCALING BEHAVIOR NEAR A CRITICAL LINE

We choose the uncoupled 1D map in two coupled 1D maps M of Eq. (2.2) as

$$u(X) = 1 - AX^2, \tag{4.1}$$

and consider a dissipative coupling case in which the coupling function is given by

$$v(X, Y) = \frac{c}{2}[u(Y) - u(X)]. \tag{4.2}$$

Here c is a coupling parameter. There exists a critical line segment associated with intermittency on the synchronous saddle-node bifurcation line $A = A_c$ in the $c - A$ plane. Inside the critical line segment, the critical behaviors are governed by the fixed point (f^*, G_I^*) with no relevant CE's, and hence they are essentially the same as those for the 1D case. On the other hand, the critical scalings near both ends are governed by the fixed point (f^*, G_{II}^*) with one relevant CE. As c passes through both ends, the coupling leads to desynchronization of the interacting systems. Hence the synchronous attractor ceases to be an attractor and a new asynchronous attractor appears outside the critical line segment. Thus a transition from a synchronous to an asynchronous state occurs at both ends of the critical line segment.

As an example, we consider the saddle-node bifurcation to a pair of synchronous orbits with period $p = 3$ occurring for $A = A_c = 1.75$. To study the intermittency associated with this bifurcation, we first consider the third iterate $M^{(3)}$ of M [see eq. (3.1)], and then shift the origin of coordinates (X, Y) to one of the three synchronous fixed points (X^*, Y^*) for $A = A_c$ [$Y^* = X^* = u^{(3)}(X^*)$]. Thus we obtain a map T of the form (3.4), where the uncoupled and coupling parts f and g are given by

$$f(x) = u^{(3)}(x + X^*) - X^*, \tag{4.3}$$

$$g(x, y) = W^{(3)}(x + X^*, y + Y^*) - u^{(3)}(x + X^*). \tag{4.4}$$

Near the region of the synchronous saddle-node bifurcation, $f(x)$ can be expanded about $x = 0$ and $A = A_c$,

$$f(x) \approx x + ax^2 + \epsilon, \tag{4.5}$$

where $a = \frac{1}{2}\partial^2 f/\partial x^2|_{x=0,\, A=A_c}$ and $\epsilon = \partial f/\partial A|_{x=0,\, A=A_c}\,(A - A_c)$. Hence this corresponds to the most common case with the tangency-order $z = 2$ [see Eq. (2.1)]. The reduced coupling function $G(x)$ of $g(x, y)$ [defined in Eq. (3.18)] is also given by

$$G(x) = \frac{e}{2}\, f'(x), \quad e = c^3 - 3c^2 + 3c. \tag{4.6}$$

Consider a pair of initial functions (f_c, G) on the synchronous saddle-node bifurcation line $A = A_c$, where $f_c(x)$ is just the 1D critical map and $G(x) = \frac{e}{2}\, f_c'(x)$. By successive actions of the reduced renormalization transformation $\tilde{\mathcal{R}}$ of Eq. (3.20) on (f_c, G), we obtain

$$f_n(x) = \alpha f_{n-1}(f_{n-1}(\frac{x}{\alpha})), \;\; G_n(x) = \frac{e_n}{2}\, f_n'(x), \tag{4.7}$$

$$e_n = 2e_{n-1} - e_{n-1}^2, \;\; (n = 0, 1, 2, \ldots), \tag{4.8}$$

where the rescaling factor for $z = 2$ is $\alpha = 2$, $f_0(x) = f_c(x)$, $G_0(x) = G(x)$, and $e_0 = e$. Here f_n converge to the 1D fixed function $f^*(x)$ of Eq. (3.16) with $z = 2$ as $n \to \infty$.

Figure 1 shows a plot of the curve determined by Eq. (4.8). Two intersection points between this curve and the straight line $e_n = e_{n-1}$ are just the fixed points e^* of the recurrence relation (4.8) for e,

$$e^* = 0,\, 1. \tag{4.9}$$

Stability of each fixed point e^* is determined by its stability multiplier λ [$= de_n/de_{n-1}|_{e^*}$]. The fixed point at $e^* = 1$ is superstable ($\lambda = 0$), while the other one at $e^* = 0$ is unstable

($\lambda = 2$). The basin of attraction to the superstable fixed point $e^* = 1$ is the open interval $(0, 2)$. That is, any initial e inside the interval $0 < e < 2$ converges to $e^* = 1$ under successive iterations of the transformation (4.8). The left end of the interval is just the unstable fixed point $e^* = 0$, which is also the image of the right end point under the recurrence equation (4.8). All the other points outside the interval diverge to the minus infinity under iterations of the transformation (4.8).

It follows from the relation $e = e(c)$ in Eq. (4.6) that there exists a critical line segment joining two end points $c_l = 0$ and $c_r = 2$ on the synchronous saddle-node bifurcation line $A = A_c$ in the $c - A$ plane. Inside the critical line segment, any initial $G(x)$ is attracted to the first reduced coupling fixed function $G_I^*(x) = \frac{1}{2} f^{*\prime}(x)$ under iterations of $\tilde{\mathcal{R}}$, while $G(x)$'s at both ends are attracted to the second reduced coupling fixed function $G_{II}^*(x) = 0$ with $b = 0$.

Figure 2 shows a phase diagram for the case of a dissipative coupling (4.2). The diagram is obtained from calculation of Lyapunov exponents. For the case of a synchronous orbit, its two Lyapunov exponents are given by

$$\sigma_\parallel(A) = \lim_{m\to\infty} \frac{1}{m} \sum_{t=0}^{m-1} \ln |u'(X_t)|, \tag{4.10}$$

$$\sigma_\perp(A, c) = \lim_{m\to\infty} \frac{1}{m} \sum_{t=0}^{m-1} \ln |(1-c)u'(X_t)| = \sigma_\parallel(A) + \ln |1-c|. \tag{4.11}$$

Here $\sigma_\parallel(\sigma_\perp)$ denotes the mean exponential rate of divergence of nearby orbits along (across) the synchronization line $Y = X$. Hereafter, $\sigma_\parallel$ ($\sigma_\perp$) will be referred to as tangential and transversal Lyapunov exponents, respectively. Note also that $\sigma_\parallel$ is just the Lyapunoiv exponent for the 1D case, and the coupling affects only $\sigma_\perp$.

The data points on the $\sigma_\perp = 0$ curve are denoted by solid circles in Fig. 2. A synchronous orbit on the synchronization line becomes a synchronous attractor with $\sigma_\perp < 0$ inside the $\sigma_\perp = 0$ curve. The type of this synchronous attractor is determined according to the sign of $\sigma_\parallel$. A synchronous period-3 orbit with $\sigma_\parallel < 0$ becomes a synchronous periodic attractor above the critical line segment, while a synchronous chaotic attractor with $\sigma_\parallel > 0$ exists below the critical line segment. The periodic and chaotic parts in the phase diagram are denoted by P and C, respectively. There exists also a synchronous period-3 attractor with $\sigma_\parallel = 0$ on the critical line segment between the two parts.

Consider a transition to chaos near an interior point with $c_l < c < c_r$ of the critical line segment. Here we fix the value of the coupling parameter c and vary the control parameter ϵ_A ($\equiv A_c - A$). For $\epsilon_A < 0$ there exists a synchronous period-3 attractor on the synchronization line $Y = X$. However, as ϵ_A is increased from zero, the periodic attractor disappears and a new chaotic attractor appears on the synchronization line. As an example, see the figure 3(a) which shows a synchronous chaotic attractor for the case $\epsilon_A = 10^{-4}$. The motion on this synchronous chaotic attractor is characterized by the occurrence of intermittent alternations between laminar and turbulent behaviors on the synchronization line, as shown in Fig. 3(b). This is just the intermittency occurring in the uncoupled 1D map, because the motion on the synchronization line is the same as that for the uncoupled 1D case. Thus, a "1D-like" intermittent transition to chaos occurs near interior points of the critical line segment.

The scaling relations of the mean duration of the laminar phase $\bar{l}$ and the tangential Lyapunov exponent $\sigma_\parallel$ for a synchronous chaotic attractor are obtained from the leading

relevant eigenvalues δ_1 $(= 4)$ of the fixed point (f^*, G_I^*) of $\tilde{\mathcal{R}}$ with no relevant CE's, like the 1D case [3]. A map with non-zero ϵ near an interior point of the critical line segment is transformed into a new map of the same form, but with a new parameter ϵ' under a renormalization transformation. Here the control parameter scales as

$$\epsilon_A' = \delta_1 \epsilon_A = 2^2 \epsilon_A. \tag{4.12}$$

Then the mean duration $\bar{l}$ and the tangential Lyapunov exponent $\sigma_\parallel$ satisfy the homogeneity relations,

$$\bar{l}(\epsilon_A') = \frac{1}{2}\bar{l}(\epsilon_A), \quad \sigma_\parallel(\epsilon_A') = 2\sigma_\parallel(\epsilon_A), \tag{4.13}$$

which lead to the scaling relations,

$$\bar{l}(\epsilon_A) \sim \epsilon_A^{-\mu}, \quad \sigma_\parallel(\epsilon_A) \sim \epsilon_A^{\mu}, \tag{4.14}$$

with exponent

$$\mu = \log 2 / \log \delta_1 = 0.5. \tag{4.15}$$

The 1D-like intermittent transition to chaos ends at both ends c_l and c_r of the critical line segment. We fix the value of the control parameter $A = A_c (= 1.75)$ and study the critical behaviors near the two end points by varying the coupling parameter c. Inside the critical line segment $(c_l < c < c_r)$, a synchronous period-3 attractor exists on the synchronization line. However, as the coupling parameter c passes through c_l or c_r, the transversal Lyapunov exponent $\sigma_\perp$ of the synchronous periodic orbit increases from zero, as shown in Fig. 4, and hence the coupling leads to desynchronization of the interacting systems. Thus the synchronous period-3 orbit ceases to be an attractor outside the critical line segment, and a new (out-of-phase) asynchronous attractor appears. This is illustrated in Fig. 5. There exist an asynchronous attractor with period 3 denoted by uptriangles for $c = -0.0001$, while an asynchronous period-6 attractor denoted by "stars" exists for $c = 2.0001$. Since the asynchronous period-3 attractor is not a symmetric one under the exchange operator σ of Eq. (2.4), there exists also its conjugate asynchronous period-3 attractor denoted by downtriangles. But the asynchronous period-6 attractor is a symmetric one under the exchange operator σ.

The critical behaviors near both ends c_l and c_r are the same. Since the transversal Lyapunov exponent $\sigma_\perp$ is equal to $\ln|1 - c|$ for $A = A_c$ [see Eq. (4.11)], it varies linearly with respect to c near both ends, (i.e., $\sigma_\perp \sim \epsilon_c$, $\epsilon_c \equiv c_l - c$ or $c - c_r$). The scaling behavior of $\sigma_\perp$ is obtained from the relevant CE δ_2 $(= 2)$ of the fixed point (f^*, G_{II}^*) of $\tilde{\mathcal{R}}$ as follows. Consider a map with non-zero ϵ_c, (but with $\epsilon_A = 0$) near both ends. It is then transformed into a new one of the same form, but with a renormalized parameter ϵ_c' under a renormalization transformation. Here the parameter ϵ_c obeys a scaling law,

$$\epsilon_c' = \delta_2 \, \epsilon_c = 2\epsilon_c. \tag{4.16}$$

Then the transversal Lyapunov exponent $\sigma_\perp$ satisfies the homogeneity relation,

$$\sigma_c(\epsilon_c') = 2\sigma_c(\epsilon_c). \tag{4.17}$$

This leads to the scaling relation,

$$\sigma_c(\epsilon_c) \sim \epsilon_c^{\nu}, \tag{4.18}$$

with exponent

$$\nu = \log 2 / \log \delta_2 = 1. \tag{4.19}$$

Like the case of interior points of the critical line segment, the scaling behavior of $\sigma_{\|}(\epsilon_A)$ for $c = c_l$ or c_r is obtained from the relevant eigenvalue δ_1 $(= 4)$ of the fixed point (f^*, G^*_{II}), and hence it also satisfies the scaling relation (4.10). The scaling behaviors of the Lyapunov exponents $\sigma_{\|}$ and $\sigma_{\perp}$ near both ends are thus determined from two relevant eigenvalues δ_1 and δ_2 of the fixed point (f^*, G^*_{II}).

V. EXTENSION TO MANY GLOBALLY-COUPLED MAPS

Recently, much attention has been paid to dynamical systems with many nonlinear elements and a global coupling, in which each element is coupled to all the other elements with equal strength. Globally-coupled systems as the extreme limit of long-range couplings are seen in broad branches of science [15]. For example, coupled nonlinear oscillators with a global coupling frequently occur in charge density waves [18], Josepson junction arrays [19], and p-n junction arrays [20]. This kind of dynamical systems with a global coupling can be also regarded as mean-field versions of dynamical systems with local short-range couplings.

Here we study the critical behavior for intermittency in many-coupled 1D maps with a global coupling. The results of two coupled maps are straightforwardly extended to the many globally-coupled maps.

A. Many globally-coupled 1D maps

Consider an N-coupled map with a periodic boundary condition:

$$\begin{aligned} M : X_{t+1}(m) &= W(\sigma^{m-1}\mathbf{X}_t) \\ &= W(X_t(m), X_t(m+1), \ldots, X_t(m-1)), \\ & \qquad\qquad m = 1, \ldots, N, \end{aligned} \tag{5.1}$$

where the number of constituent elements N is a positive integer larger than or equal to 2, $X_t(m)$ is the state of the mth element at a lattice point m and at a discrete time t, $\mathbf{X} = (X(1), X(2), \ldots, X(N))$, σ is the cyclic permutation of the elements of $\mathbf{X}$, i.e., $\sigma\mathbf{X} = (X(2), \ldots, X(N), X(1))$, σ^{m-1} means $(m-1)$ applications of σ. The periodic condition imposes $X_t(m) = X_t(m+N)$ for all m. Like the two-coupled case $(N = 2)$, the function W consists of two parts:

$$W(\mathbf{X}) = u(X(1)) + v(\mathbf{X}), \tag{5.2}$$

where u is an uncoupled 1D map and v is a coupling function obeying the condition,

$$v(X,\ldots,X)=0 \quad \text{for any } X. \tag{5.3}$$

Thus the N-coupled map (5.1) becomes:

$$\begin{aligned} M: X_{t+1}(m) &= u(X_t(m)) \\ &\quad +v(X_t(m),X_t(m+1),\ldots,X_t(m-1)), \\ &\quad m=1,\ldots,N. \end{aligned} \tag{5.4}$$

Here we study many-coupled 1D maps with a global coupling. In the extreme long-range case of global coupling, the coupling function v is of the form,

$$v(X(1),\ldots,X(N))=\frac{c}{N}\sum_{m=1}^{N}[r(X(m))-r(X(1))] \ \text{ for } N\geq 2, \tag{5.5}$$

where $r(X)$ is a function of one variable. Note that each 1D map is coupled to all the other ones with equal coupling strength c/N inversely proportional to the number of degrees of freedom N. Hereafter, c will be called the coupling parameter.

The N-coupled map M is called a symmetric map, because it has a cyclic permutation symmetry such that

$$\sigma^{-1}M\sigma(\mathbf{X})=M(\mathbf{X}) \ \text{ for all } \mathbf{X}, \tag{5.6}$$

where σ^{-1} is the inverse of σ. The set of all fixed points of σ forms a synchronization line in the N-dimensional state space, on which

$$X(1)=\cdots=X(N). \tag{5.7}$$

It follows from Eq. (5.6) that the cyclic permutation σ commutes with the symmetric map M, i.e., $\sigma M=M\sigma$. Hence the synchronization line becomes invariant under M. An orbit is called a(n) (in-phase) synchronous orbit if it lies on the synchronization line, i.e., it satisfies

$$X_t(1)=\cdots=X_t(N)\equiv X_t^* \ \text{ for all } t. \tag{5.8}$$

Otherwise, it is called an (out-of-phase) asynchronous orbit. Here we study the intermittency associated with a synchronous saddle-node bifurcation. Note also that synchronous orbits can be easily found from the uncoupled 1D map, $X_{t+1}^*=u(X_t^*)$, because of the coupling condition (5.3).

B. Lyapunov exponents of synchronous orbits and the critical behavior

Consider an orbit $\{\mathbf{X}_t\}\equiv\{X_t(m),\, m=1,\ldots,N\}$ in many coupled maps (5.4). Stability analysis of the orbit can be easily carried out by Fourier transforming with respect to the discrete space $\{m\}$. The discrete spatial Fourier transform of the orbit is:

$$\begin{aligned} \mathcal{F}[X_t(m)]\equiv\frac{1}{N}\sum_{m=1}^{N}e^{-2\pi imj/N}\,X_t(m)=\xi_t(j), \\ j=0,1,\ldots,N-1. \end{aligned} \tag{5.9}$$

The Fourier transform $\xi_t(j)$ satisfies $\xi_t^*(j) = \xi_t(N-j)$ ($*$ denotes complex conjugate), and the wavelength of a mode with index j is $\frac{N}{j}$ for $j \le \frac{N}{2}$ and $\frac{N}{N-j}$ for $j > \frac{N}{2}$. Here $\xi_t(0)$ corresponds to the synchronous (Fourier) mode of the orbit, while all the other $\xi_t(j)$'s with nonzero indices j correspond to the asynchronous (Fourier) modes.

To determine the stability of a synchronous orbit $[X_t(1) = \cdots = X_t(N) \equiv X_t^*$ for all $t]$, we consider an infinitesimal perturbation $\{\Delta X_t(m)\}$ to the synchronous orbit, i.e., $X_t(m) = X_t^* + \Delta X_t(m)$ for $m = 1, \ldots, N$. Linearizing the N-coupled map (5.4) at the synchronous orbit, we obtain:

$$\Delta X_{t+1}(m) = u'(X_t^*)\Delta X_t(m) + \sum_{l=1}^{N} V^{(l)}(X_t^*)\Delta X_t(l+m-1), \tag{5.10}$$

where

$$u'(X) = \frac{du}{dx}, \quad V^{(l)}(X) \equiv \left.\frac{\partial v(\sigma^{(m-1)}\mathbf{X})}{\partial X_{l+m-1}}\right|_{X(1)=\cdots=X(N)=X} = \left.\frac{\partial v(\mathbf{X})}{\partial X_l}\right|_{X(1)=\cdots=X(N)=X}. \tag{5.11}$$

Hereafter, the functions $V^{(l)}$'s will be called "reduced coupling functions" of $v(\mathbf{X})$.

Let $\delta\xi_t(j)$ be the Fourier transform of $\Delta X_t(m)$, i.e.,

$$\delta\xi_t(j) = \mathcal{F}[\Delta X_t(m)] = \frac{1}{N}\sum_{m=1}^{N} e^{-2\pi i m j/N}\,\Delta X_t(m), \quad j = 0, 1, \ldots, N-1. \tag{5.12}$$

Here $\delta\xi_t(0)$ is the synchronous-mode perturbation along the synchronization line, while all the other ones $\delta\xi_t(j)$'s with nonzero indicies j are the asynchronous-mode perturbations across the synchronization line. Then the Fourier transform of Eq. (5.10) becomes:

$$\delta\xi_{t+1}(j) = [u'(X_t^*) + \sum_{l=1}^{N} V^{(l)}(X_t^*)e^{2\pi i(l-1)j/N}]\,\delta\xi_t(j), \quad j = 0, 1, \ldots, N-1. \tag{5.13}$$

Note that all the modes $\xi_t(j)$'s become decoupled for the synchronous orbit.

The Lyapunov exponent λ_j of a synchronous orbit, characterizing the average exponential rate of divergence of the jth-mode perturbation, is given by

$$\sigma_j = \lim_{m\to\infty}\frac{1}{m}\sum_{t=0}^{m-1} \ln|u'(X_t^*) + \sum_{l=1}^{N} V^{(l)}(X_t^*)e^{2\pi i(l-1)j/N}|. \tag{5.14}$$

If the Lyapunov exponent σ_j is negative or zero, then the synchronous orbit is stable against the jth-mode perturbation; otherwise it is unstable.

In case of a synchronous periodic orbit with period p, the Lyapunov exponent σ_j in Eq. (5.14) becomes:

$$\sigma_j = \frac{1}{p} \ln |\lambda_j|, \tag{5.15}$$

where λ_j, called the stability multiplier of the synchronous orbit, is given by

$$\lambda_j = \prod_{t=0}^{p-1} [u'(X_t^*) + \sum_{l=1}^{N} V^{(l)}(X_t^*) e^{2\pi i (l-1) j/N}]. \tag{5.16}$$

The synchronous periodic orbit is stable against the jth-mode perturbation when λ_j lies inside the unit circle, i.e., $|\lambda_j| < 1$. When the stability multiplier λ_j increases through 1, the synchronous periodic orbit loses its stability via saddle-node or pitchfork bifurcation. On the other hand, when λ_j decreases through -1, it becomes unstable via period-doubling bifurcation.

It follows from the coupling condition (5.3) that

$$\sum_{l=1}^{N} V^{(l)}(X) = 0. \tag{5.17}$$

Hence the Lyapunov exponent σ_0 becomes

$$\sigma_0 = \lim_{m\to\infty} \frac{1}{m} \sum_{t=0}^{m-1} \ln |u'(X_t^*)|. \tag{5.18}$$

It is just the Lyapunov exponent of the uncoupled 1D map. While there is no coupling effect on σ_0, coupling generally affects the other Lyapunov exponents σ_j's ($j \neq 0$).

In case of the global coupling of the form (5.5), the reduced coupling functions become:

$$V^{(l)}(X) = \begin{cases} (1-N)V(X) & \text{for } l = 1, \\ V(X) & \text{for } l \neq 1, \end{cases} \tag{5.19}$$

where

$$V(X) = \frac{c}{N} r'(X). \tag{5.20}$$

Substituting $V^{(l)}$'s into Eq. (5.14), we obtain:

$$\sigma_j = \begin{cases} \lim_{m\to\infty} \frac{1}{m} \sum_{t=0}^{m-1} \ln |u'(X_t^*)| \text{ for } j = 0, \\ \lim_{m\to\infty} \frac{1}{m} \sum_{t=0}^{m-1} \ln |u'(X_t^*) - cr'(X_t^*)| \text{ for } j \neq 0. \end{cases} \tag{5.21}$$

Here σ_0 is just the tangential Lyapunov exponent $\sigma_\parallel$ of Eq. (4.10), characterizing the mean exponential rate of divergence of nearby orbits along the synchronization line (5.8). On the other hand, all the other ones σ_j ($j \neq 0$) (characterizing the mean exponential rate of divergence of nearby orbits across the synchronization line) are the same as the transversal Lyapunov exponent $\sigma_\perp$ of Eq. (4.11), i.e.,

$$\sigma_1 = \cdots = \sigma_{N-1} = \sigma_\perp. \tag{5.22}$$

Consequently, there exist only one independent transversal Lyapunov exponent $\sigma_\perp$.

As for the case of two coupled maps in Sec. IV, we choose $u(X) = 1 - AX^2$ as the uncoupled 1D map, and consider a global-coupling case with $r(X) = u(X)$, i.e., a global-coupling of the form

$$v(X(1), \ldots, X(N)) = \frac{c}{N} \sum_{m=1}^{N} [u(X(m)) - u(X(1))] \text{ for } N \geq 2. \tag{5.23}$$

[Here the case for $N = 2$ is just the dissipative coupling of Eq. (4.2).] For this kind of global coupling, the transversal Lyapunov exponent (5.22) is given by

$$\sigma_\perp = \sigma_\parallel + \ln|1 - c|. \tag{5.24}$$

As in Sec. IV, we also consider the intermittency associated with a saddle-node bifurcation to a pair of synchronous periodic orbits with period 3. Then the phase diagram in Fig. 2 holds for all N ($N \geq 2$) globally-coupled maps, because the two independent Lyapunov exponents $\sigma_\parallel$ and $\sigma_\perp$ are the same, irrespectively of N. Thus there exists a critical line segment joining two ends $c_l = 0$ and $c_r = 2$ on the synchronous saddle-node-bifurcation line $A = A_c = 1.75$ in the $c - A$ plane for any N globally-coupled case. The critical behaviors of N globally-coupled maps for $N > 2$ are also essentially the same as those of two dissipatively-coupled maps, in which case there are two kinds of critical behaviors (for details of the $N = 2$ case, refer to Sec. IV).

C. Renormalization analysis of many globally-coupled maps

As seen in Sec. V B, there exists the same critical line segment associated with intermittency for N ($N = 2, 3, 4, \ldots$) globally-coupled maps, irrespectively of N. Following the same procedure of Sec. III for two coupled maps, we extend the renormalization results of two coupled maps to arbitrary N globally-coupled maps. We thus find two fixed maps of the reduced renormalization transformation and obtain their relevant eigenvalues. One fixed map with no relevant CE's is associated with the critical behavior inside the critical line segment, while the other one with relevant CE's is associated with the critical behavior at both ends.

To study the intermittency in the vicinity of a saddle-node bifurcation to a pair of synchronous orbits with period p in an N-coupled map M of Eq. (5.1), consider its pth iterate $M^{(p)}$,

$$\begin{aligned} M^{(p)} : X_{t+1}(m) &= W^{(p)}(\sigma^{m-1}\mathbf{X}_t) \\ &= W^{(p)}(X_t(m), X_t(m+1), \ldots, X_t(m-1)), \\ &\qquad m = 1, \ldots, N, \end{aligned} \tag{5.25}$$

where $W^{(p)}$ satisfies a recurrence relation

$$W^{(p)}(\mathbf{X}) = W(W^{(p-1)}(\mathbf{X}), W^{(p-1)}(\sigma\mathbf{X}), \ldots, W^{(p-1)}(\sigma^{N-1}\mathbf{X})), \tag{5.26}$$

and it can be also decomposed into two parts, the uncoupled part $u^{(p)}$ and the remaining coupling part, i.e.,

$$W^{(p)}(\mathbf{X}) = u^{(p)}(X(1)) + [W^{(p)}(\mathbf{X}) - u^{(p)}(X(1)]. \tag{5.27}$$

For the threshold value A_c of a synchronous saddle-node bifurcation, p synchronous fixed points of $M^{(p)}$ appear. Shifting the origin of coordinates $(X(1), \ldots, X(N))$ to one of the p fixed points $(X^*(1), \ldots, X^*(N))$ $(X^*(1) = \cdots = X^*(N) \equiv X^* = u^{(p)}(X^*)$ for $A = A_c)$, we have

$$\begin{aligned} T : x_{t+1}(m) &= F(\sigma^{m-1}\mathbf{x}_t)) \\ &= f(x_t(m)) + g(x_t(m), \ldots, x_t(m-1)), \\ &\qquad m = 1, \ldots, N, \end{aligned} \tag{5.28}$$

where

$$f(x(1)) = u^{(p)}(x(1) + X^*) - X^*, \tag{5.29}$$

$$g(\mathbf{x}) = W^{(p)}(x(1) + X^*, \ldots, x(N) + X^*) - u^{(p)}(x(1) + X^*). \tag{5.30}$$

Here $\mathbf{x} = (x_1, \ldots, x_N)$, the uncoupled part f for the critical case $A = A_c$ satisfies the condition (3.7), and the coupling function also obeys the condition (5.3).

We employ the same renormalization transformation $\mathcal{N}$ of Eq. (3.9) with the rescaling operator αI, where α is a rescaling factor, and I is the $N \times N$ identity matrix. Applying the renormalization operator $\mathcal{N}$ to the N-coupled map (5.28) n times, we obtain the n-times renormalizaed map T_n of the form,

$$\begin{aligned} T_n : x_{t+1}(m) &= F_n(\sigma^{m-1}\mathbf{x}_t) \\ &= f_n(x_t(m)) + g_n(x_t(m), \ldots, x_t(m-1)), \\ &\qquad m = 1, \ldots, N. \end{aligned} \tag{5.31}$$

Here the uncoupled and coupling parts f and g satisfy the following recurrence relations:

$$f_{n+1}(x(1)) = \alpha f_n(f_n(\frac{x(1)}{\alpha})), \tag{5.32}$$

$$\begin{aligned} g_{n+1}(\mathbf{x}) = {} & \alpha f_n(F_n(\frac{\mathbf{x}}{\alpha})) + \alpha g_n(F_n(\frac{\mathbf{x}}{\alpha}), \ldots, F_n(\frac{\sigma^{N-1}\mathbf{x}}{\alpha})) \\ & -\alpha f_n(f_n(\frac{x(1)}{\alpha})). \end{aligned} \tag{5.33}$$

Then Eqs. (5.32) and (5.33) define a renormalzation operator $\mathcal{R}$ of transforming a pair of functions (f, g):

$$\begin{pmatrix} f_{n+1} \\ g_{n+1} \end{pmatrix} = \mathcal{R} \begin{pmatrix} f_n \\ g_n \end{pmatrix}. \tag{5.34}$$

A critical map T_c is attracted to a fixed map T^* under iterations of the renormalization transformation $\mathcal{N}$,

$$\begin{aligned} T^* : x_{t+1}(m) &= F^*(\sigma^{m-1}\mathbf{x}_t) \\ &= f^*(x_t(m)) \\ &\quad + g^*(x_t(m), x_t(m+1), \ldots, x_t(m-1)), \\ &\qquad m = 1, \ldots, N. \end{aligned} \tag{5.35}$$

Here (f^*, g^*) is a fixed point of the renormalization operator $\mathcal{R}$, i.e., $(f^*, g^*) = \mathcal{R}(f^*, g^*)$. Since f^* is just the 1D fixed map (3.16), only the equation for the coupling fixed function g^* is left to be solved.

As in case of two coupled maps, we construct a tractable recurrence equation for a reduced coupling function of $g(\mathbf{x})$ defined by

$$G^{(l)}(x) = \left.\frac{\partial g(\mathbf{x})}{\partial x(l)}\right|_{x(1)=\cdots=x(N)=x}, \tag{5.36}$$

because it is not easy to directly solve the equation for the coupling fixed function. Differentiating the recurrence equation (5.33) for g with respect to $x(l)$ $(l = 1, \ldots, N)$ and setting $x(1) = \cdots = x(n) = x$, we obtain:

$$\begin{aligned} G^{(l)}_{n+1} = & f_n'(f_n(\frac{x}{\alpha}))\, G^{(l)}_n(\frac{x}{\alpha}) \\ & + G^{(l)}_n(f_n(\frac{x}{\alpha}))\, f_n'(\frac{x}{\alpha}) \\ & + \sum_{i=1}^{N} G^{(i)}_n(f_n(\frac{x}{\alpha}))\, G^{(l-i+1)}_n(\frac{x}{\alpha}). \end{aligned} \tag{5.37}$$

The reduced coupling functions $G^{(l)}$'s satisfy the sum rule (5.17), i.e., $\sum_{l=1}^{N} G^{(l)}(x) = 0$, and they also satisfy $G^{(l)}(x) = G^{(l+N)}(x)$ due to the periodic boundary condition.

As shown in Eq. (5.19), there exists only one independent reduced coupling function $G(x)$ for the globally-coupled case, such that

$$\begin{aligned} & G^{(2)}(x) = \cdots = G^{(N)}(x) \equiv G(x), \\ & G^{(1)}(x) = (1 - N)G(x). \end{aligned} \tag{5.38}$$

Then it is easy that the successive images $\{G^{(l)}_n(x)\}$ of $\{G^{(l)}(x)\}$ under the transformation (5.37) also satisfy Eq. (5.38) [i.e., $G^{(2)}_n = \cdots = G^{(N)}_n(x) \equiv G_n(x)$, $G^{(1)}_n(x) = (1 - N)G_n(x)$]. Consequently, there remains only one recurrence equation for the independent reduced coupling function $G(x)$ [10]:

$$\begin{aligned} G_{n+1}(x) = & [f_n'(f_n(\frac{x}{\alpha})) - N G_n(f_n(\frac{x}{\alpha}))] G_n(\frac{x}{\alpha}) \\ & + G_n(f_n(\frac{x}{\alpha})) f_n'(\frac{x}{\alpha}). \end{aligned} \tag{5.39}$$

Then, together with Eq. (5.32), Eq. (5.39) defines a reduced renormalization operator $\tilde{\mathcal{R}}$ of transforming a pair of functions (f, G):

$$\begin{pmatrix} f_{n+1} \\ G_{n+1} \end{pmatrix} = \tilde{\mathcal{R}} \begin{pmatrix} f_n \\ G_n \end{pmatrix}. \tag{5.40}$$

Since the reduced renormalization transformation (5.40) holds for any globally-coupled cases of $N \geq 2$, it can be regarded as a generalized version of Eq. (3.20) for the case of two coupled maps.

A pair of critical functions (f_c, G) is attracted to a pair of fixed functions (f^*, G^*) under iterations of $\tilde{\mathcal{R}}$. Here f^* is the 1D fixed map (3.16), and $G^*(x)$ is the independent reduced coupling fixed-function of $g^*(\mathbf{x})$ [i.e., $G^{*(2)}(x) = \cdots = G^{*(N)}(x) = G^*(x)$, $G^{*(1)}(x) = (1 - N)G^*(x)$]. As in the two-coupled case ($N = 2$) of Eqs. (3.21) and (3.22), we find two series solutions for G^*:

$$G^*_I(x) = \frac{1}{N}[1 + zax^{z-1} + z(z - \frac{1}{2})a^2x^{2(z-1)} + \cdots], \tag{5.41}$$

$$G^*_{II}(x) = \frac{1}{N}[bax^{z-1} + b(\frac{3z - b}{2} - \frac{1}{2})a^2x^{2(z-1)} + \cdots]. \tag{5.42}$$

Here a and b are arbitrary constants. The solutions for G^* have a common factor $\frac{1}{N}$, and hence the function $N\,G^*(x)$ becomes the same, independently of N; this can be also easily understood by looking at the structure of Eq. (5.39). In case of $G^*_I(x)$, we can sum the series and obtain a closed-form solution,

$$G^*_I(x) = \frac{1}{N}f'^*(x). \tag{5.43}$$

However, unfortunately we cannot sum the series in $G^*_{II}(x)$ except for the cases $b = 0$ and z where we obtain closed-form solutions,

$$G^*_{II}(x) = \begin{cases} 0 & \text{for } b = 0, \\ \frac{1}{N}[f^{*\prime}(x) - 1] & \text{for } b = z. \end{cases} \tag{5.44}$$

Linearizing the renormalization transformation $\tilde{\mathcal{R}}$ at its fixed point (f^*, G^*), we obtain a reduced linearized operator $\tilde{\mathcal{L}}$ transforming a pair of infinitesimal perturbations (h, Φ):

$$\begin{pmatrix} h_{n+1} \\ \Phi_{n+1} \end{pmatrix} = \tilde{\mathcal{L}} \begin{pmatrix} h_n \\ \Phi_n \end{pmatrix} = \begin{pmatrix} \tilde{\mathcal{L}}_1 & 0 \\ \tilde{\mathcal{L}}_3 & \tilde{\mathcal{L}}_2 \end{pmatrix} \begin{pmatrix} h_n \\ \Phi_n \end{pmatrix}, \tag{5.45}$$

where

$$h_{n+1}(x) = [\tilde{\mathcal{L}}_1 h_n](x) = \alpha f^{*\prime}(f^*(\frac{x}{\alpha}))h_n(\frac{x}{\alpha}) + \alpha h_n(f^*(\frac{x}{\alpha})), \tag{5.46}$$

$$\Phi_{n+1}(x) = [\tilde{\mathcal{L}}_2\Phi_n](x) + [\tilde{\mathcal{L}}_3 h_n](x), \tag{5.47}$$

$$[\tilde{\mathcal{L}}_2\Phi_n](x) = [f^{*\prime}(f^*(\frac{x}{\alpha})) - NG^*(f^*(\frac{x}{\alpha}))]\Phi_n(\frac{x}{\alpha}) + [f^{*\prime}(\frac{x}{\alpha}) - NG^*(\frac{x}{\alpha})]\Phi_n(f^*(\frac{x}{\alpha})), \tag{5.48}$$

$$\begin{aligned}[\tilde{\mathcal{L}}_3 h_n](x) = {} & [f^{*\prime\prime}(f^*(\frac{x}{\alpha}))G^*(\frac{x}{\alpha}) - NG^{*\prime}(f^*(\frac{x}{\alpha}))G^*(\frac{x}{\alpha}) + G^{*\prime}(f^*(\frac{x}{\alpha}))f^{*\prime}(\frac{x}{\alpha})]h_n(\frac{x}{\alpha}) \\ & + G^*(\frac{x}{\alpha})h'_n(f^*(\frac{x}{\alpha})) + G^*(f^*(\frac{x}{\alpha}))h'_n(\frac{x}{\alpha}).\end{aligned} \tag{5.49}$$

It follows from the reducibility of $\tilde{\mathcal{L}}$ into a semiblock form that to determine the eigenvalues of $\tilde{\mathcal{L}}$ it is sufficient to solve the eigenvalue problems for $\tilde{\mathcal{L}}_1$ and $\tilde{\mathcal{L}}_2$ independently. Then the eigenvalues of both $\tilde{\mathcal{L}}_1$ and $\tilde{\mathcal{L}}_2$ give the whole spectrum $\tilde{\mathcal{L}}$.

The eigenvalue equation for $\tilde{\mathcal{L}}_1$ is given by Eq. (3.31). As mentioned there, that is just the eigenvalue equation for the 1D map, in which case the complete spectrum of eigenvalues and the corresponding eigenfunctions have been found in Refs. [3].

We next consider an infinitesimal coupling-perturbation of the form $(0, \Phi)$ to a fixed point (f^*, G^*). If an independent reduced coupling perturbation Φ^* satisfies

$$\begin{aligned}\lambda\Phi^*(x) &= [\tilde{\mathcal{L}}_2\Phi^*](x) \\ &= [f^{*\prime}(f^*(\frac{x}{\alpha})) - NG^*(f^*(\frac{x}{\alpha}))]\Phi^*(\frac{x}{\alpha}) \\ &\quad +[f^{*\prime}(\frac{x}{\alpha}) - NG^*(\frac{x}{\alpha})]\Phi^*(f^*(\frac{x}{\alpha})),\end{aligned} \tag{5.50}$$

then it is called the independent reduced coupling eigenfunction with CE λ. Note that the eigenvalue equation (5.50) for any N becomes the same as that for the two-coupled case ($N = 2$), because the function $NG^*(x)$ is the same, irrespectively of N. Hence we follow the same procedure in Sec. III for two coupled maps, and find the same relevant CE's for any N globally-coupled maps as follows (for more details, refer to Sec. III):

$$\begin{aligned}&(1)\ G^*(x) = G^*_I(x) \\ &\quad \text{There exist no relevant CE}'\text{s.} \qquad (5.51) \\ &(2)\ G^*(x) = G^*_{II}(x) \\ &\quad \text{There exist } (z-1) \text{ relevant CE}'\text{s such that } \lambda_k = 2^{(z-1-k)/(z-1)} \\ &\quad \text{with eigenfunction } \Phi^*_k(x) \text{ of Eq. (3.37) } (k = 0, \ldots, z-2). \qquad (5.52)\end{aligned}$$

As in Sec. V B, we also consider the global coupling of Eq. (5.23) with $r(X) = u(X) = 1 - AX^2$ and study the intermittency associated with a saddle-node bifurcation to a pair of synchronous orbits with period $p = 3$. Considering the third iterate $M^{(3)}$ of M [see Eq. (5.25)] and then shifting the origin of coordinates to one of the three synchronous fixed points for $A = A_c$, we obtain a map of the form T (5.28). The uncoupled part f has the form (4.5), ans hence that corresponds to the most common case with the tangency-order $z = 2$. The independent reduced coupling function of the coupling part $g(\mathbf{x})$ is also given by

$$G(x) = \frac{e}{N} f'(x),\ e = c^3 - 3c^2 + 3c. \tag{5.53}$$

Consider a pair of initial functions (f_c, G) on the synchronous saddle-node bifurcation line $A = A_c$, where $f_c(x)$ is just the 1D critical map and $G(x) = \frac{e}{N} f'_c(x)$. By successive applications of the reduced renormalization operator $\tilde{\mathcal{R}}$ of Eq. (5.40) to (f_c, G), we have

$$f_n(x) = \alpha f_{n-1}(f_{n-1}(\frac{x}{\alpha})),\ \ G_n(x) = \frac{e_n}{N} f'_n(x) \tag{5.54}$$

$$e_n = 2e_{n-1} - e^2_{n-1}, \tag{5.55}$$

where the rescaling factor for $z = 2$ is $\alpha = 2$, $f_0(x) = f_c(x)$, $G_0(x) = G(x)$, and $e_0 = e$. Here f_n converge to the 1D fixed function $f^*(x)$ of Eq. (3.16) with $z = 2$ as $n \to \infty$.

As shown in Sec. IV, any initial e inside the open interval $(0, 2)$ converges to the super-stable fixed point $e^* = 1$ under successive iterations of the transformation (5.55). The left end of the interval is un unstable fixed point $e^* = 0$, which is also the image of the right end $e = 2$ under the transformation (5.55); all the other points outside the interval diverges to the minus infty under iterations of the transformation (5.55). One can see easily that the interval $[0, 2]$ of the parameter e corresopnds to a critical line segment joining two ends

$c_l = 0$ and $c_r = 2$ on the synchronous saddle-node bifurcation line $A = A_c$ in the $c - A$ plane. Hence any initial $G(x)$ inside the critical line segment is attracted to the first independent reduced coupling fixed function $G^*_I(x) = \frac{1}{N} f^*(x)$ under iterations of $\tilde{\mathcal{R}}$, while $G(x)'s$ at both ends are attracted to the second independent reduced coupling fixed function $G^*_{II}(x) = 0$ with $b = 0$.

VI. SUMMARY

The critical behaviors for intermittency in two coupled 1D maps are studied by a renormalization method. We find two fixed maps of the renormalization transformation. Although they have common relevant eigenvalues associated with scaling of the control parameter of the uncoupled 1D map, their relevant CE's associated with coupling perturbations vary depending on the fixed maps. These two fixed maps are also found to be associated with the critical behavior near a critical line segment. One fixed map with relevant CE's govern the critical behavior at both ends of the critical line segment, while the other one with no relevant CE's governs the critical behavior inside the critical line segment. We also extend the results of the two coupled 1D maps to many globally-coupled 1D maps.

ACKNOWLEDGMENTS

This work was supported by the the Korea Research Foundation under Project No. 1997-001-D00099.

REFERENCES

[1] P. Manneville and Y. Pomeau, Phys. Lett. A **75**, 1 (1979); Physica D **1**, 219 (1980); Y. Pomeau and P. Manneville, Commun. Math. Phys. **74**, 189 (1980).

[2] J-P Eckmann, L. Thomas and P. Wittwer, J. Phys. A **14**, 3153 (1981); J. E. Hirsh, B. A. Hubermann and D. J. Scalapino, Phys. Rev. A **25**, 519 (1982).

[3] J. E. Hirsh, M. Nauenberg, and D. J. Scalapino, Phys. Lett. A **87**, 391 (1982); B. Hu and J. Rudnick, Phys. Rev. Lett. **48**, 1645 (1982).

[4] M. J. Feigenbaum, J. Stat. Phys. **19**, 25 (1978); **21**, 669 (1979).

[5] I. Waller and R. Kapral, Phys. Rev. A **30**, 2047 (1984); R. Kapral, Phys. Rev. A **31**, 3868 (1985).

[6] S. P. Kuznetsov, Radiophys. Quantum Electron. **28**, 681 (1985); S. P. Kuznetsov and A. S. Pikovsky, Physica D **19**, 384 (1986); H. Kook, F. H. Ling, and G. Schmidt, Phys. Rev. A **43**, 2700 (1991).

[7] I. S. Aranson, A. V. Gaponov-Grekhov and M. I. Rabinovich, Physica D **33**, 1 (1988).

[8] S.-Y. Kim and H. Kook, Phys. Rev. A **46**, R4467 (1992).

[9] S.-Y. Kim and H. Kook, Phys. Lett. A **178**, 258 (1993).

[10] S.-Y. Kim and H. Kook, Phys. Rev. E **48**, 785 (1993).

[11] S.-Y. Kim, Phys. Rev. E **49**, 1745 (1994).

[12] K. Kaneko, in *Theory and Applications of Coupled Map Lattices*, edited by K. Kaneko (John Willy & Sons, New York, 1992), p. 1, and references cited therein.

[13] S.-Y. Kim and K. Lee, Phys. Rev. E **54**, 1237 (1996).

[14] S.-Y. Kim, Phys. Rev. E **52**, 1206 (1995); Phys. Rev. E **54**, 3393 (1996).

[15] K. Kaneko, Phys. Rev. Lett. **63**, 219 (1989); Physica D **41**, 137 (1990); Phys. Rev. Lett. **65**, 1391 (1990); Physica D **55**, 368 (1992).

[16] J. Guckenheimer and P. Holmes, *Nonlinear Oscillations, Dynamical Systems, and Bifurcations of Vector Fields* (Springer-Verlag, New York, 1983), Sec. 3.5.

[17] See Appendix A of Ref. [10].

[18] P. Alstrøm and R. K. Ritala, Phys. Rev. A **35**, 300 (1987).

[19] P. Hadley, M. R. Beasley, and K. Wiesenfeld, Phys. Rev. B **38**, 8712 (1988); K. Wiesenfeld and P. Hadley, Phys. Rev. Lett. **62**, 1335 (1988); S. Nichols and K. Wiesenfeld, Phys. Rev. A **45**, 8430 (1992).

[20] L. Fabiny and K. Wiesenfeld, Phys. Rev. A **43**, 2640 (1991).

FIGURES

FIG. 1. Plots of the curve $e_n = 2e_{n-1} - e_{n-1}^2$ and the straight line $e_n = e_{n-1}$.

FIG. 2. Phase diagram for a dissipative-coupling case (4.2). Here solid circles denote the data points on the $\sigma_\perp = 0$ curve. The region enclosed by the $\sigma_\perp = 0$ curve is divided into two parts dnoted by P and C. A synchronous period-3 (chaotic) attractor with $\sigma_\parallel < 0$ ($\sigma_\parallel > 0$) exists in the part P (C). The boundary curve denoted by a solid line between the P and C parts is just the critical line segment.

FIG. 3. Iterates of the dissipatively-coupled map M of Eq. (2.2) with the uncoupled 1D map (4.1) and the coupling (4.2) for ϵ_A $(= A_c - A) = 10^{-4}$ and $c = 0.5$; (a) an orbit with initial point $(0.1, 0.3)$ is attracted to a synchronous chaotic attractor on the synchronization line $Y = X$ after exhibiting a short transient behavior, and (b) the plot of the X-component $X_t^{(3)}$ of the third iterate $M^{(3)}$ of M versus a discrete time t shows intermittent alternations between laminar and turbulent behaviors.

FIG. 4. Plot of $\sigma_\perp$ $(= \ln|1 - c|)$ versus c for $A = A_c$. The values of $\sigma_\perp$ at both ends of the critical line segment are zero, which are denoted by solid circles.

FIG. 5. Transition from a synchronous to an asynchronous state for $A = A_c$. A synchronous period-3 orbit denoted by circles is no longer an attractor outside the critical line segment, and new asynchronous attractors exist for (a) $c = -0.0001$ and (b) $c = 2.0001$. We denote a pair of asynchronous period-3 attractors by uptriangles and downtriangles in case of (a), while the asynchronous attrractor with period 6 is denoted by "stars" in case of (b).

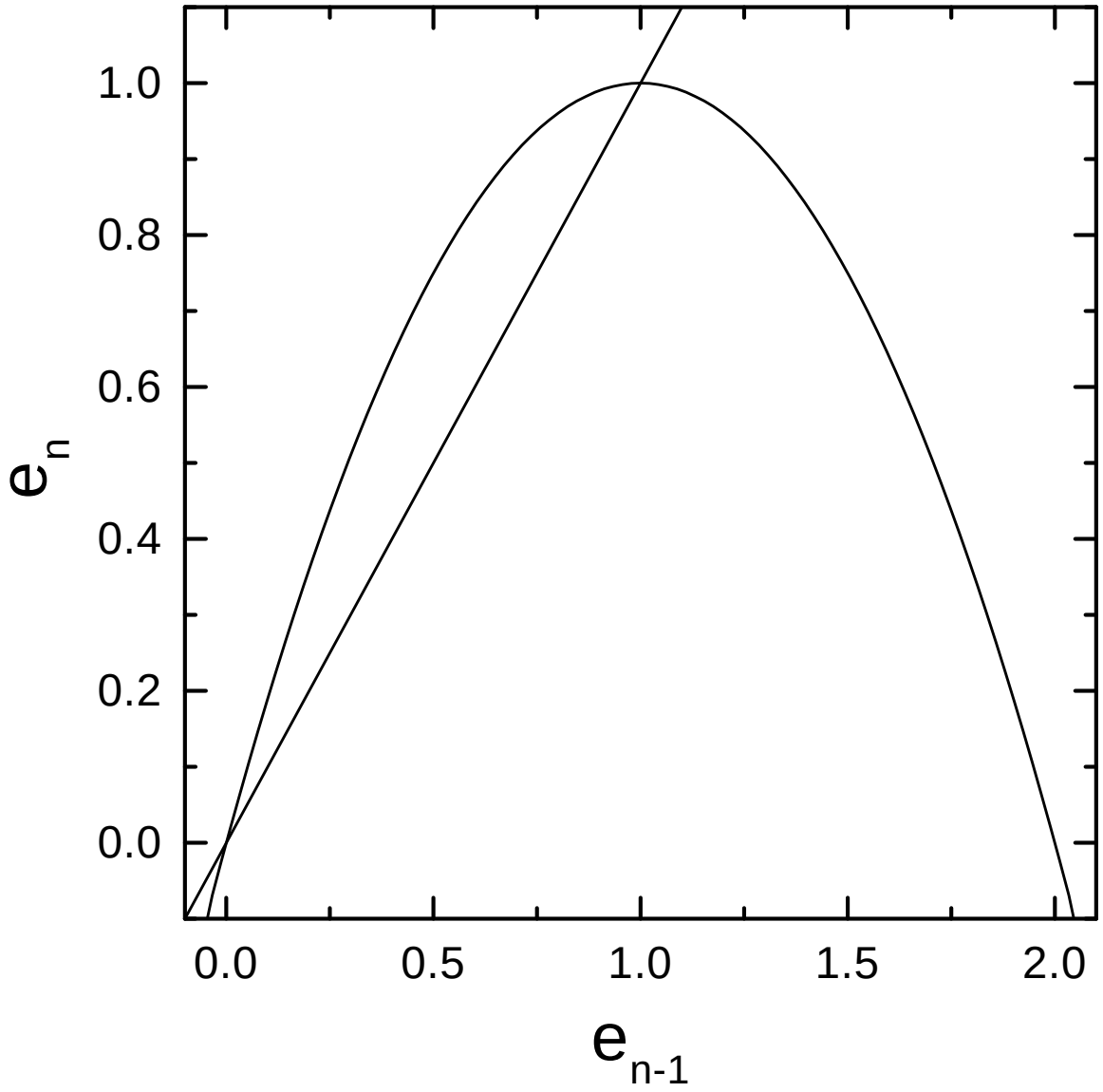

Fig. 1 (Kim,PR-E)

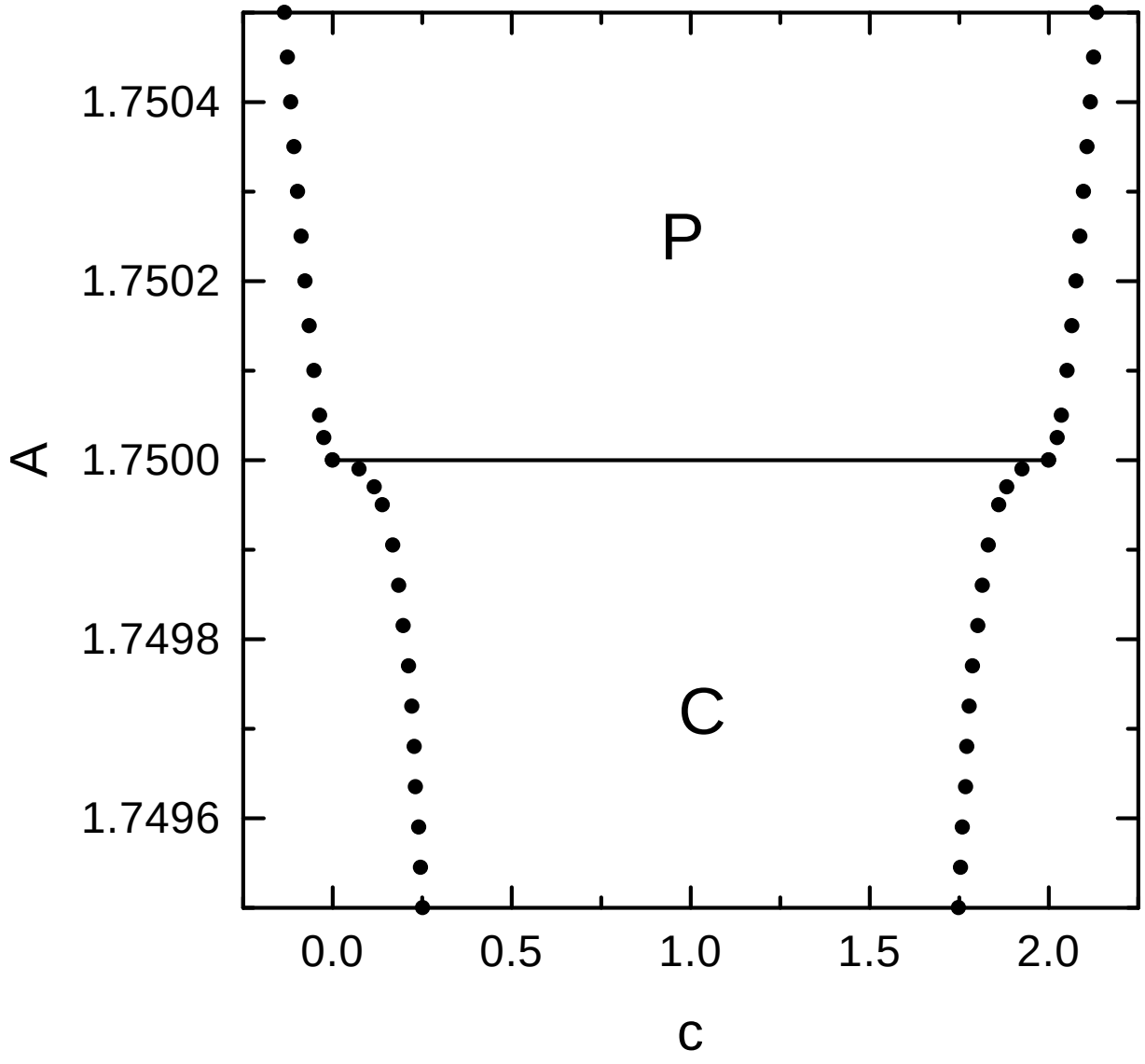

Fig. 2 (Kim,PR-E)

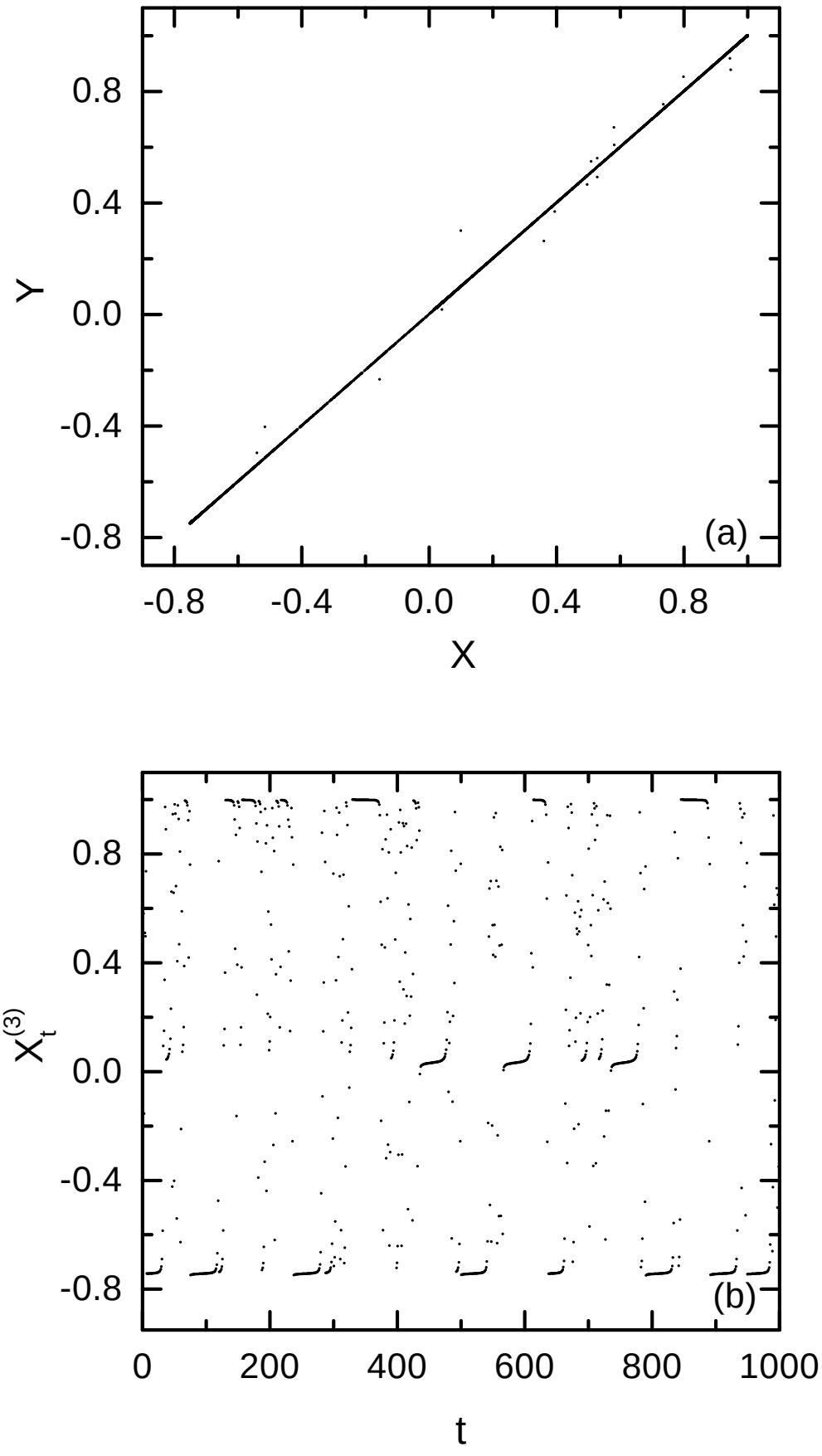
0.8
0.4
0.0
-0.4
-0.8
Y
(a)
-0.8
-0.4
0.0
0.4
0.8
X
0.8
0.4
0.0
-0.4
-0.8
$X_t^{(3)}$
(b)
0
200
400
600
800
1000
t

Fig. 3 (Kim,PR-E)

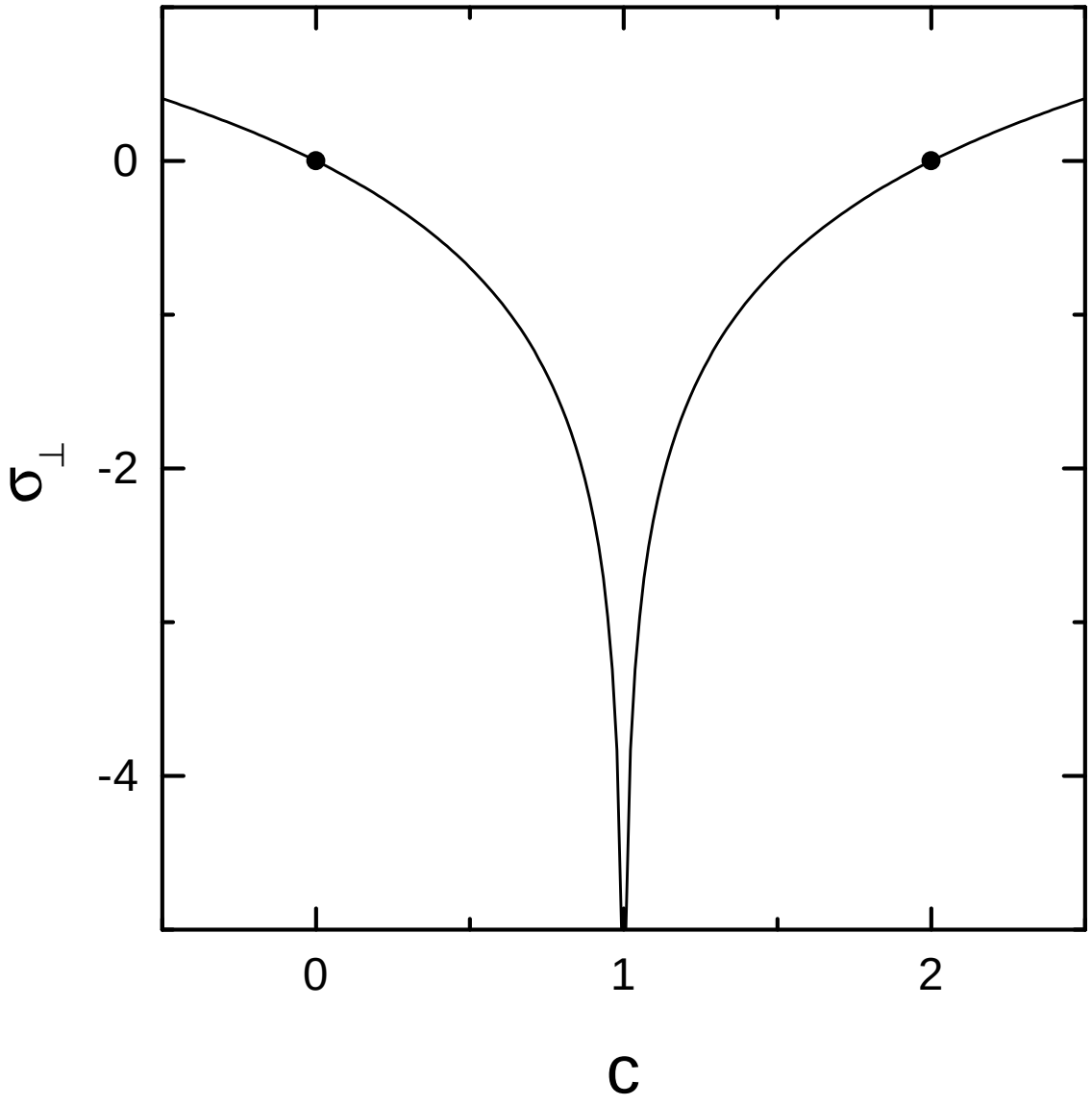

Fig. 4 (Kim,PR-E)

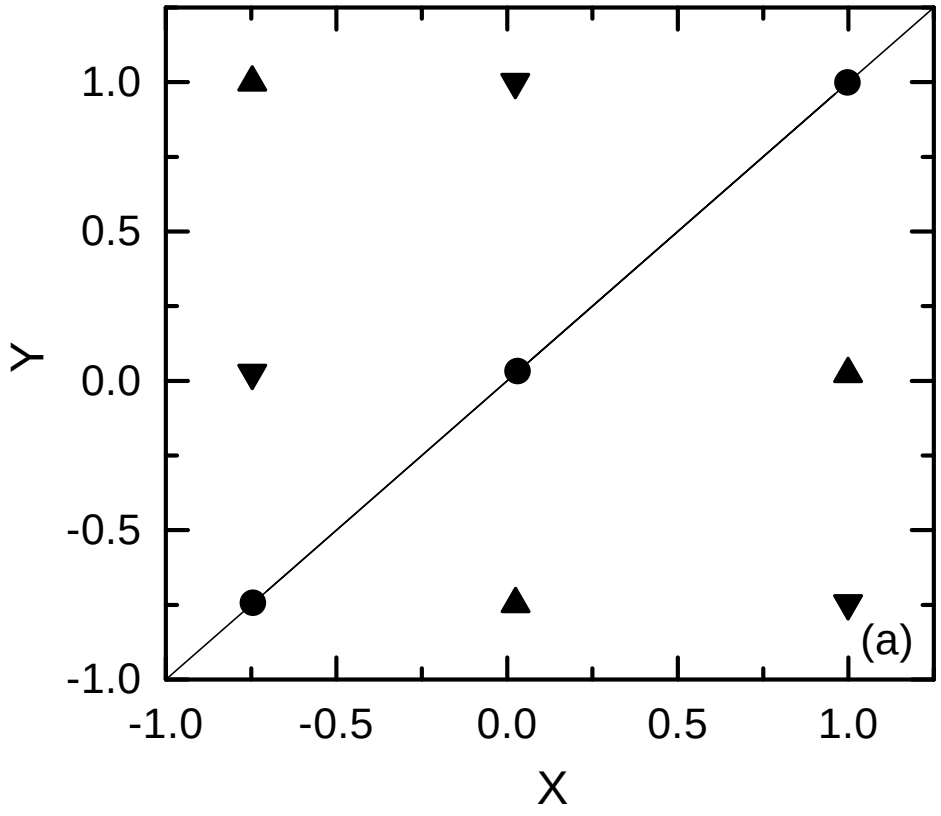

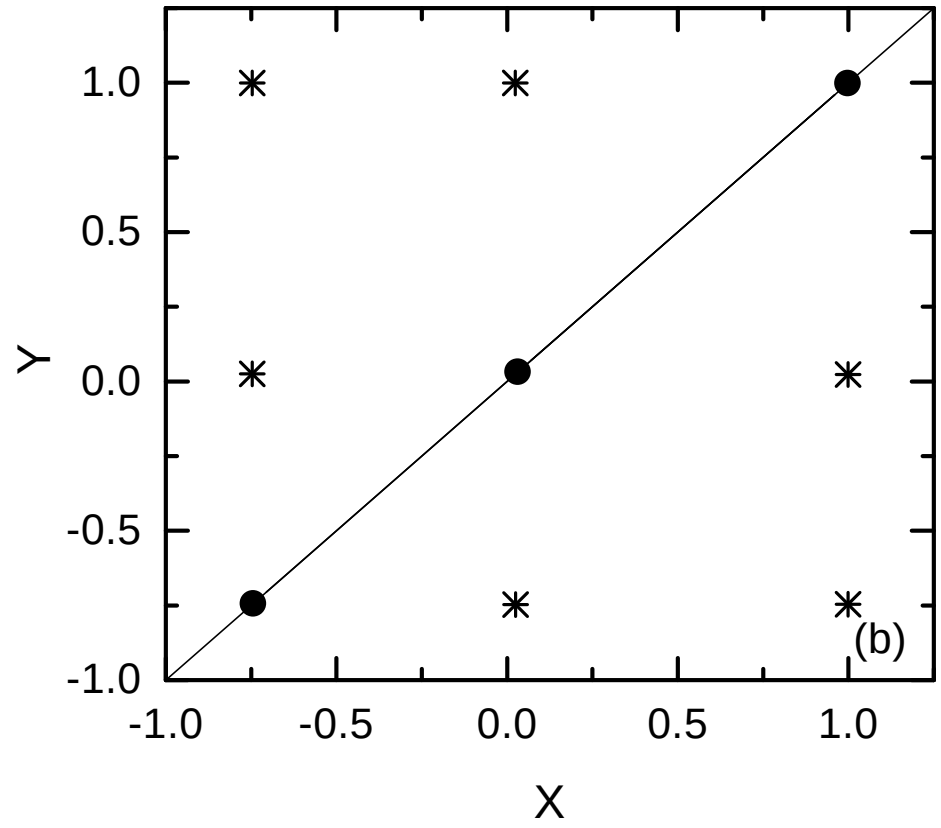

Fig. 5 (Kim,PR-E)